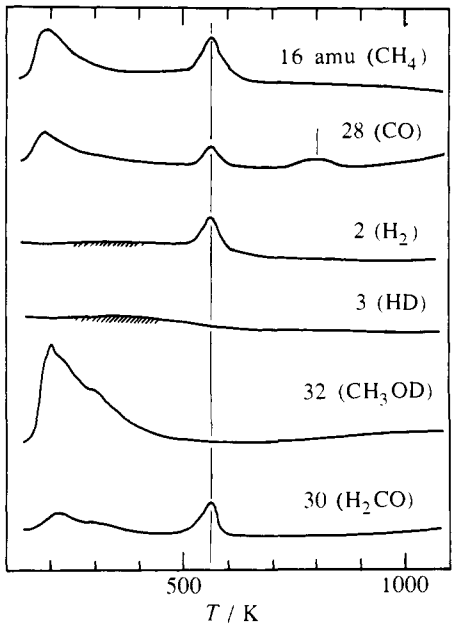

Figure 3. TPD traces measured after exposure of Mo(112)-p(1×2)-O at 130 K to 4 langmuirs of CH_3OD.

coordinated by one O(a) atom (Mo_{1C}), and those not coordinated (Mo_{NC}), the ratio of the three being 1:2:1. Considering the van der Waals radius[5] of O atoms, it is expected that CO cannot be adsorbed on Mo_{2C} but can be adsorbed on Mo_{1C} and Mo_{NC}. The α_1- and α_2-CO species are then assigned to CO adsorbed on Mo_{NC} and Mo_{1C}, respectively. This assignment applies also to CO TPD from p(1×2)-O, where Mo_{NC} and Mo_{4C} coexist and only α_1-CO is observed.

The desorption energies of α_1- and α_2-CO are estimated to be 72 and 56 kJ mol^{-1}, respectively.[6] The difference, 16 kJ mol^{-1}, is ascribed to the electronic effect of one O modifier, since the steric blocking is negligible for Mo_{1C}. This electronic effect is restricted to Mo atoms directly coordinated by O(a) and can be explained in terms of the withdrawal of electrons by electronegative O(a). On the other hand, the gradual shift of the CO desorption peaks, from 310 to 280 K for α_1, is ascribed to a long-range electronic effect due to the rearrangement of surface electronic states extending to several lattice spacings.[7]

The TPD measurement after exposure of clean Mo(112) at 130 K to CH_3OD showed desorption-limited peaks of HD and H_2 at 380 K and a sharp desorption peak of H_2 at 410 K, suggesting that CH_3OD dissociates to methoxy (CH_3O(a)) and D(a) at low temperatures. D(a) is recombinatively desorbed with H(a) adsorbed from the residual gas. CH_3O(a) is decomposed at 410 K to form H_2(g), C(a), and O(a). The C(a) and O(a) species are desorbed above 800 K as CO, in contrast to the cases of many transition metal surfaces,[8] where the reaction-limited, simultaneous desorption of CO and H_2 is observed. A small amount of CH_4 is also desorbed at 450 K. These results indicate that the C-O bond scission competes well with the C-H scission on clean Mo(112).

A remarkably different reaction path is opened on p(1×2)-O, whereas the TPD results for p(2×1)-O are practically identical to those for clean Mo(112). Figure 3 shows TPD measured after exposure of the p(1×2)-O surface to CH_3OD. Simultaneous desorption of H_2CO, H_2, CO, and CH_4 is observed at 560 K, below which only hydrogen desorbs at 300-400 K. The desorption at 560 K does not contain deuterated species, indicating that CH_3O(a) is formed also on p(1×2)-O at low temperatures and is decomposed at 560 K. The shift of the decomposition temperature by 150 K suggests the stabilization of CH_3O(a) on p(1×2)-O.

On molybdenum oxide catalysts, the oxidative dehydrogenation of CH_3OH occurs to form H_2CO and H_2O.[9,10] By contrast, a dehydrogenation path to produce H_2CO and H_2 is newly opened on Mo(112)-p(1×2)-O. The desorbed products from p(1×2)-^{18}O did not contain ^{18}O-labeled species, indicating that O(a) plays only a role as a modifier. The amount of C(a) and O(a) formed during the methoxy decomposition was small compared with the case of low-θ_O surfaces, suggesting that the C-O bond scission is restrained on p(1×2)-O. We suggest that the CH_3O(a) decomposition on p(1×2)-O is triggered by the C-H scission, since the simultaneous desorption peaks shifted upward by 10 K when CD_3OD was used. The CO adsorption experiments indicated that the electronic structure of top-layer Mo_{NC} atoms is identical for both p(2×1)-O and p(1×2)-O. The suppression of the C-O bond scission on p(1×2)-O is then ascribed to the steric blocking by O(a) of second-layer Mo, which plays an essential role in the C-O bond cleavage.

Registry No. Mo, 7439-98-7; CO, 630-08-0; O, 17778-80-2; CH_3OH, 67-56-1; molybdenum oxide, 11098-99-0.

(5) Bondi, A. *J. Phys. Chem.* **1964**, *68*, 441.
(6) The preexponential factor for desorption was assumed to be 10^{13} s^{-1}.
(7) Feibelman, P. J.; Hamann, D. R. *Phys. Rev. Lett.* **1984**, *52*, 61.
(8) Parmeter, J. E.; Jiang, X.; Goodman, D. W. *Surf. Sci.* **1990**, *240*, 85 and references therein.
(9) Farneth, W. E.; Ohuchi, F.; Staley, R. H.; Chowdhry, U.; Sleight, A. W. *J. Phys. Chem.* **1985**, *89*, 2493.
(10) Iwasawa, Y. *Adv. Catal.* **1987**, *35*, 87.

Stereoselective Hydrogen-Transfer Reactions Involving Acyclic Radicals. A Study of Radical Conformations Using Semiempirical Calculations

K. Durkin and D. Liotta*

Department of Chemistry, Emory University
1515 Pierce Drive, Atlanta, Georgia 30322

J. Rancourt,[†] J.-F. Lavallée,[†] L. Boisvert,[‡] and Y. Guindon[†,‡]

Bio-Méga Inc., 2100 rue Cunard
Laval, Québec, Canada H7S 2G5
Department of Chemistry, Université de Montréal
Montréal, Québec, Canada H3C 3J7

Received February 20, 1992

Stereoselectivity in intermolecular reactions of acyclic free radicals is a topic of current interest in chemical literature.[1] Recent reports show that chirality transfer can be achieved using stereogenic centers adjacent to a radical center.[2-4] The theoretical interpretation of these results being at an early stage, we have been developing a transition-state model that would account for the stereocontrol noted when radicals of low SOMO energy are

[†] Bio-Méga Inc.
[‡] Université de Montréal.
(1) Porter, N. A.; Giese, B.; Curran, D. P. *Acc. Chem. Res.* **1991**, *24*, 296 and references cited therein.
(2) (a) Hart, D. J.; Huang, H.-C. *Tetrahedron Lett.* **1985**, *26*, 3749. (b) Hart, D. J.; Krishnamurthy, R. *Synlett* **1991**, 412. (c) Hart, D. J.; Huang, H.-C.; Krishnamurthy, R.; Schwartz, T. *J. Am. Chem. Soc.* **1989**, *111*, 7507. (d) Hart, D. J.; Krishnamurthy, R. Submitted for publication (personal communication).
(3) (a) Bullard, M.; Zeitz, H.-G.; Giese, B. *Synlett* **1991**, 423. (b) Giese, B.; Bullard, M.; Zeitz, H.-G. *Synlett* **1991**, 425. (c) Crich, D.; Davies, J. W. *Tetrahedron* **1989**, *45*, 5641. (d) Ogura, K.; Yanagisawa, A.; Fujino, T.; Takahashi, K. *Tetrahedron Lett.* **1988**, *29*, 5387. (e) Crich, D.; Davies, J. W. *Tetrahedron Lett.* **1987**, *28*, 4205. (f) Vassen, R.; Runsink, J.; Scharf, H.-D. *Chem. Ber.* **1986**, *119*, 3492. (g) Henning, R.; Urbach, H. *Tetrahedron Lett.* **1983**, *24*, 5343. (h) Curran, D. P.; Thoma, G. *Tetrahedron Lett.* **1991**, *32*, 6307. (i) Curran, D. P.; Abraham, A. C.; Liu, H. *J. Org. Chem.* **1991**, *56*, 4335. (j) For the addition of tris(trimethylsilyl)silyl radicals to chiral ketones, see: Giese, B.; Damm, W.; Dickhaut, J.; Wetterich, F.; Sun, S.; Curran, D. P. *Tetrahedron Lett.* **1991**, *32*, 6097. (k) Arya, P.; Lesage, M. Submitted for publication (personal communication).
(4) (a) Guindon, Y.; Yoakim, C.; Lemieux, R.; Boisvert, L.; Delorme, D.; Lavallée, J.-F. *Tetrahedron Lett.* **1990**, *31*, 2845. (b) Guindon, Y.; Lavallée, J.-F.; Boisvert, L.; Chabot, C.; Delorme, D.; Yoakim, C.; Hall, D.; Lemieux, R.; Simoneau, B. *Tetrahedron Lett.* **1991**, *32*, 27. (c) For examples of chelation-controlled radical reductions, see: Guindon, Y.; Lavallée, J.-F.; Llinas-Brunet, M.; Horner, G.; Rancourt, J. *J. Am. Chem. Soc.* **1991**, *113*, 9701.

0002-7863/92/1514-4912$03.00/0

Table I. Reduction of α-Halo Ester **1** with Bu_3SnH

entry	structure	R	R^1	R^2	X	ratio threo:erythro	yield (%)
1	**1a**	Et	Me	Ph	OMe	32:1	90
2	**1b**	Et	Me	Ph	Me	2:1	85
3	**1c**	Et	Me	Ph	F	20:1	88
4	**1d**	Et	Me	Me	OMe	3:1	53
5	**1e**	Et	Me	C_6H_{11}	OMe	12:1	78
6	**1f**	Me	Me	C_6F_5	OMe	12:1	89
7	**1g**	Me	H	Ph	OMe	4:1	83
8	**1h**	Me	Me	Ph	OMe	>25:1	86
9	**1i**	Me	*i*Pr	Ph	OMe	24:1	87
10	**1j**	Me	*t*Bu	Ph	OMe	6:1	94

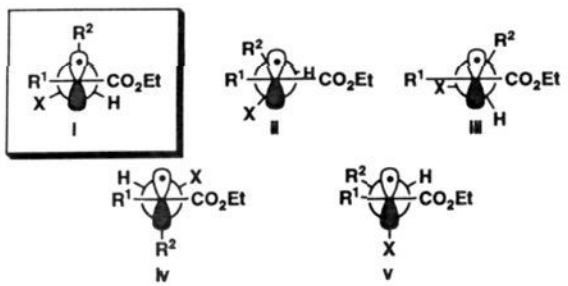

Figure 1.

involved in hydrogen-transfer reactions such as that depicted in eq 1. In this communication, we report the results of calculations which help to explain the source of stereoselection in these radical reactions. New experimental data providing a basis for better understanding of steric and electronic factors are disclosed as well.

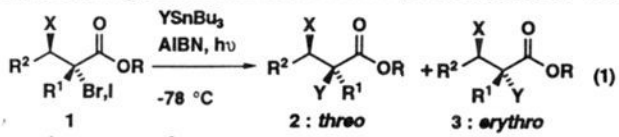

R^1 = H, alkyl; R^2 = alkyl, aryl; X = OMe, F, Me; Y = H or D

The radicals are typically generated from the corresponding bromide or iodide by reaction with Bu_3SnH at −78 °C using photochemical initiation. Of particular interest in this study was the requirement of an electronegative group (X) adjacent to the radical center to achieve significant levels of stereoselection (Table I, entries 1–3).[4] The steric influence of R^2 was also important to the stereochemical outcome of the reaction (entries 4 and 5).[4a] Interestingly, the impressive ratio of >25:1 obtained when R^2 = phenyl was reduced to 12:1 when R^2 = pentafluorophenyl (entries 6 and 8). The effect of steric hindrance at R^1 on the observed stereoselection was also examined. We noted an increase in stereoselection as R^1 was changed from hydrogen to methyl or isopropyl but not when R^1 was changed from hydrogen to a *tert*-butyl moiety (entries 7–10).

Several models of preferred radical conformations have recently been proposed (Figure 1). In these models, the radical (stabilized by delocalization) is considered to be coplanar with the ester carbonyl.[5] An early transition state for hydrogen delivery in which attack occurs from the least hindered face of the radical is apparently operative, and thus the conformational preference of the radical should strongly influence the final stereoselection. Model **i**[4b,c,6,7] is consistent with our results both in terms of steric and electronic factors. In this model, both allylic 1,3 strain and electrostatic repulsions are minimized without the presence of eclipsing interactions between R^1 and the electronegative group X. The orientation of R^2 coplanar with the radical center is also

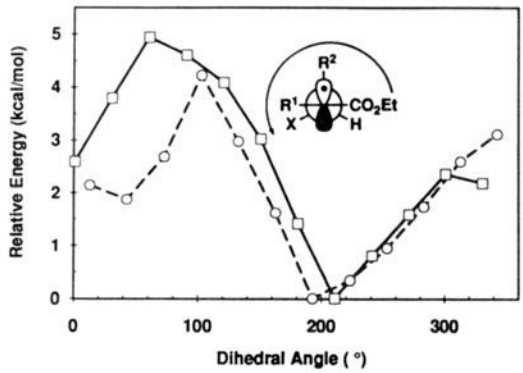

Figure 2. Typical plots of energy surfaces of radicals generated from α-halo esters as a function of the CO_2Et–C–C–X dihedral angle. Curves for radicals derived from **1a** (□) (ratio >25:1) and **1d** (○) (ratio 3:1) are shown.

suggestive of potential stabilization of the radical by hyperconjugation.[8] Model **ii** suggests conformational control via minimization of allylic strain only.[3b] Although predictive of the stereochemical outcome of the reaction (when $R^2 > X$), this model cannot account for the impressive stereoselection noted when X = F (entry 3) since the steric difference between hydrogen and fluorine is small. In model **iii**, the major source of conformational stabilization resides in minimization of intramolecular electrostatic repulsions by maintaining an anti orientation of the electronegative groups.[4a,b] Model **iii** suffers from eclipsing interactions between X and R^1 and is inconsistent with experimental results (entries 7–10) obtained when the steric nature of R^1 is changed (vide supra).[9]

We have conducted a study using semiempirical calculations to assess the conformational preference of the radical species.[10] Our calculations[11,12] utilized a dihedral driver approach with MOPAC 5.0[13] using the AM1 Hamiltonian (RHF/DOUBLET).[14] This method gave us a picture of the two-dimensional potential surface associated with rotation about the bond in question (Figure 2). In the cases described in Table I for which there was experimentally observed selectivity (entries 1, 3, 5, 8, and 9), the calculations indicated a pronounced preference for the conformation depicted in model **i**.[15] The less selective systems (Table I, entries 2, 4, and 10) exhibited at least a second mininum (Figure 2) corresponding to rotamer **iv** (±30°) and selecting for

(5) (a) Barnabas, M. V.; Venkateswaran, K.; Walker, D. C. *J. Am. Chem. Soc.* **1990**, *112*, 7163. (b) Ruchardt, C.; Beckhaus, H.-D. *Top. Curr. Chem.* **1985**, *88*, 1. (c) Bordwell, F. G.; Harrelson, J. A., Jr. *Can. J. Chem.* **1990**, *68*, 1714.

(6) This model is analogous to the one proposed by Hart in his pioneering work on acyclic radicals when X is the medium-sized substituent.[2]

(7) This rotamer was considered by Porter, Curran, and Giese as part of the "dynamic model".[1]

(8) Le Noble, W. J.; Bodepudi, V. R. *J. Org. Chem.* **1991**, *56*, 2001.

(9) As was indicated by one of our referees, some systems discussed in ref 3b do not follow the "pattern" described here. These systems correspond to radicals derived from **1** where R^1 = neopentyl, R^2 = Me, and X = $OSiMe_3$, $OSiMe_2$(*t*-Bu), $OSiPh_2$(*t*-Bu). The conformational surfaces of these systems are difficult to assess adequately by molecular orbital methods.

(10) We also considered the assumptions regarding the reactivity of these systems. We examined the transition state of the reaction of **i** (derived from **1a**) with silane to produce the threo adduct. The transition state was located and characterized by one negative force constant (Gradient Norm < 2) and was found to occur at an Si–H bond distance of 1.58 Å and a C–H bond length of 1.56 Å with an activation energy of 12.18 kcal/mol. Our results correlate well with the view of these systems as having an early transition state and validate the concept of a rotamer-based model to predict qualitatively the selectivity of these simple systems.

(11) MMX (PCMODEL) optimized geometries were used as input for all molecular orbital studies. All calculations were done on Silicon Graphics 4D/35 and IBM 550 workstations. MOPAC optimized geometries were dihedral driven about the C–C bond between the radical carbon and the stereogenic carbon in 30° increments. All other bond lengths, angles, and dihedrals for each structure were fully optimized with MOPAC at the given (fixed) dihedral value. The output of each dihedral value is used as the input for the next dihedral step.

(12) Gilbert, K.; Gajewski, R. *Advances in Molecular Modeling*; Liotta, D., Ed.; JAI Press Inc.: Greenwich, CT, 1990; Vol. 2. We are grateful to Kevin Gilbert of Serene Software for making this program available to us.

(13) Stewart, J. J. P. *J. Comp. Aided Mol. Des.* **1990**, *4*, 1 (QCPE program No. 455).

(14) Dewar, M. J. S.; Zoebisch, E. G.; Healy, E. F.; Stewart, J. J. P. *J. Am. Chem. Soc.* **1985**, *107*, 3902.

(15) (a) Calculations indicate that product **1g** should show strong stereoselectivity, but this is not noted experimentally (entry 7). (b) Systems having highly flexible substituents (for example when X = OMOM, OAc) were least well described by this approach.

the erythro adduct.[16] An increase in the depth of this minimum *qualitatively* correlated with a decrease in the ratio of observed adducts. If allylic 1,3 interactions were the most important controlling factor, one would have predicted that conformer v was the source of the erythro products. Apparently stabilization through σ donation (and minimization of $A_{1,2}$ interactions in the electron-poor radical) compensates for the destabilizing dipole–dipole and allylic 1,3 effects present in conformer iv.

One of our most interesting results involved the experimental observation that pentafluorophenyl system **1f** delivered only about half of the selectivity of phenyl system **1h**. Quantitatively this result could not have been predicted by our calculations although qualitatively there is a profound difference between the two cases. Pentafluoro compound **1f** shows an equivalent energy of conformers located between 210° and 260°, which is suggestive of other controlling factors such as through-space interactions or changes in the σ donating ability of R^2, aspects that we are currently studying. We are also performing a theoretical evaluation of the transition states involved in the reaction, and ESR studies are presently being conducted in order to confirm experimentally the conformational preferences indicated by our calculations.

Acknowledgment. A Natural Sciences and Engineering Research Council of Canada (NSERC) Industrial Research Fellowship (J.R.) is gratefully acknowledged. Ab initio calculations were performed by Dr. W. Cui. The authors thank Dr. W. Ogilvie for assistance during the preparation of this manuscript.

Supplementary Material Available: A listing of experimental procedures and spectral data (^{1}H NMR, ^{13}C NMR, IR, MS, and/or HRMS) for compounds **1–3** as well as calculation data (12 pages). Ordering information is given on any current masthead page.

(16) GAUSSIAN 90 calculations were also performed on the radical derived from **1d**. Ab initio SCF at UHF/6-31G*//3-21G was used; Frisch, M. J.; Head-Gordon, M.; Trucks, G. W.; Foresman, J. B.; Schlegel, H. B.; Raghavachari, K.; Robb, M. A.; Binkley, J. S.; Gonzalez, C.; Defrees, D. J.; Fox, D. J.; Whiteside, R. A.; Seeger, R.; Melius, C. F.; Baker, J.; Martin, R. L.; Kahn, L. R.; Stewart, J. J. P.; Topiol, S.; Pople, J. A. Guassian Inc., Pittsburgh, PA, 1990. Rotamer i was again identified as being the most stable rotamer. It is interesting to note that MNDO did not reproduce these effects, instead generating a rotamer in which the ester was twisted out of plane with respect to the radical carbon.

Synthesis and Structural Characterization of a Hybrid Triazene–Thiaborane Cluster: (μ_2(4,*exo*-9)-1-SiMe$_3$-3-H-N$_3$)-*arachno*-6-SB$_9$H$_{10}$

Stefan Küpper,[1] Patrick J. Carroll, and Larry G. Sneddon*

Department of Chemistry
University of Pennsylvania
Philadelphia, Pennsylvania 19104-6323

Received February 21, 1992

Azide compounds have proven to be valuable building blocks for the synthesis of boron nitrogen compounds. Early investigations focused on the reaction of azides with compounds containing classically bonded borons,[2,3] but recently azide reactions have also been employed for the synthesis of polyhedral azaborane clusters.[4,5] For example, the reaction of HN_3 with $B_{10}H_{12}(SMe_2)_2$ was found to yield *nido*-$NB_{10}H_{13}$ by way of an azido(μ-amino)decaborane intermediate.[4a]

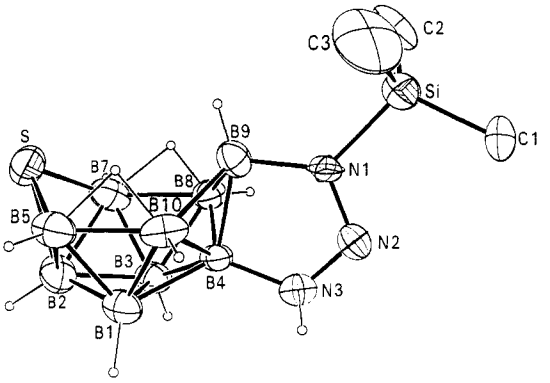

Figure 1. ORTEP drawing of the molecular structure of (μ_2(4,*exo*-9)-1-SiMe$_3$-3-H-N$_3$)-*arachno*-6-SB$_9$H$_{10}$. (The hydrogen atoms on the trimethylsilyl group are not shown.) Selected bond lengths (Å) and angles (deg): S–B5, 1.874 (11); S–B7, 1.921 (10); B4–B9, 1.698 (10); B7–B8, 1.815 (12); B5–B10, 1.849 (14); B8–B9, 1.921 (13); B9–B10, 1.917 (11); B4–N3, 1.486 (10); B9–N1, 1.515 (10); N2–N3, 1.283 (7); N1–N2, 1.292 (8); B9–B4–N3, 97.2 (5); B4–N3–N2, 118.2 (6); N1–N2–N3, 110.7 (5); N2–N1–B9, 115.0 (5); N1–B9–B4, 98.8 (6).

These previous results suggested that other classes of polyhedral boranes, and in particular the polyhedral thiaboranes, might also be susceptible to similar insertion reactions to yield previously unknown hybrid (μ-amino)thiaboranes or thiaazaboranes. We report here that *nido*-6-SB$_9$H$_{11}$ reacts readily with an organic derivative of hydrazoic acid, trimethylsilyl azide, to give the first example[6] of a new class of hybrid fused-ring cluster triazene–thiaborane compounds, (μ_2(4,*exo*-9)-1-SiMe$_3$-3-H-N$_3$)-*arachno*-6-SB$_9$H$_{10}$ (**1**).

nido-6-SB$_9$H$_{11}$ + Me$_3$SiN$_3$ → (μ_2(4,*exo*-9)-1-SiMe$_3$-3-H-N$_3$)-*arachno*-6-SB$_9$H$_{10}$ (**1**)

In a typical reaction, 5.36 g of *arachno*-$Me_4N^+SB_9H_{12}^-$ (25 mmol), 3.15 g of I_2 (12.5 mmol), and 50 mL of toluene were used to generate *nido*-6-SB$_9$H$_{11}$ as described previously.[7] The solution was filtered into a second flask, and an excess of trimethylsilyl azide (3.6 g, 31 mmol) was added dropwise at room temperature. This solution was then heated at reflux for approximately 3 h. The solvent was removed and the remaining oily residue dissolved in ether, filtered, and recrystallized. Sublimation at 80 °C/10^{-3} Torr, and recrystallization afforded 2.7 g (10.5 mmol) of **1**[8] as a white powder in 42% nonoptimized yield.

In contrast to free triazenes,[9] **1** exhibits both thermal and photolytic stability. For example, no nitrogen was evolved nor any decomposition observed upon xylene reflux for 3 days or upon photolysis in toluene solution for 3 h.

The structure of (μ_2(4,*exo*-9)-1-SiMe$_3$-3-H-N$_3$)-*arachno*-6-SB$_9$H$_{10}$, as determined by a single-crystal X-ray study, is shown in the ORTEP drawing in Figure 1.[10] The cage framework is

(1) Present address: Institut für Anorganische Chemie der RWTH Aachen, Prof. Pirlet Strasse 1, 5100 Aachen, Germany.

(2) Paetzold, P. *Adv. Inorg. Chem.* **1987**, *31*, 123–170.

(3) (a) Paetzold, P.; Redenz-Stormanns, B.; Boese, R. *Angew. Chem., Int. Ed. Engl.* **1991**, *29*, 900–902. (b) Tapper, A.; Schmitz, T.; Paetzold, P. *Chem. Ber.* **1989**, *122*, 595–601.

(4) (a) Müller, J.; Paetzold, P.; Boese, R. *Heteroat. Chem.* **1990**, *1*, 461–465. (b) Müller, J.; Runsink, J.; Paetzold, P. *Angew. Chem., Int. Ed. Engl.* **1991**, *30*, 175.

(5) Paetzold, P. *Pure Appl. Chem.* **1991**, *63*, 345–350.

(6) Fused organic-ring/carborane or metallacarborane clusters have been reported. See, for example: (a) Hota, N. K.; Matteson, D. S. *J. Am. Chem. Soc.* **1968**, *90*, 3570–3572. Matteson, D. S.; Hota, N. K. *J. Am. Chem. Soc.* **1971**, *93*, 2893–2897. (b) Miller, V. R.; Weiss, R.; Grimes, R. N. *J. Am. Chem. Soc.* **1977**, *99*, 5646–5651. Pipal, J. R.; Grimes, R. N. *Inorg. Chem.* **1978**, *17*, 10–14. (c) Wu, S.-h.; Jones, M., Jr. *Inorg. Chem.* **1988**, *27*, 2004–2008.

(7) Rudolph, R. W.; Pretzer, W. R. *Inorg. Synth.* **1983**, *22*, 226–229.

(8) Spectroscopic data: IR (KBr pellet) 3370 (s), 2960 (w), 2910 (w), 2550 (s), 2530 (s), 1460 (w), 1345 (m), 1255 (m), 1000 (m), 850 (s), 840 (s); ^{11}B-NMR (64.2 MHz, in $CDCl_3$) (ppm, Hz) 7.4 (s, B4), −6.0 (d, B5,7, J_{BH} 149), −8.3 (d, B9, J_{BH} 136), −19.9 (d, B2, J_{BH} 183), −38.7 (d, B8–10, J_{BH} 136), −40.3 (d, B1–3, J_{BH} 143). Two-dimensional ^{11}B–^{11}B-COSY-NMR established the following connectivities: B1,3–B2, –B4, –B5,7, –B8,10; B4–B9, –B8,10; B9–B8,10; ^{1}H-NMR (200 MHz, $CDCl_3$) (ppm) 10.36 (1 H, NH), 0.48 (9 H, SiMe$_3$), −1.7 (2 H, μH); exact mass calcd for $^{12}C_3{}^1H_{20}{}^{11}B_9{}^{14}N_3{}^{32}S^{28}Si$ 257.1985, found 257.2018; mp 116 °C. Anal. Calcd C, 14.09; H, 7.89; N, 16.44. Found: C, 13.49; H, 7.80; N, 15.56.

(9) Wiberg, N. *Adv. Organomet. Chem.* **1985**, *24*, 179–248.

0002-7863/92/1514-4914$03.00/0